New calculations of the PNC Matrix Element for the $J^\pi T$ $0^+1, 0^-1$ doublet in ^{14}N

Mihai Horoi* **and Günther Clausnitzer**

Strahlenzentrum der Justus-Liebig-Universität, D-6300 Giessen, Germany

B. Alex Brown

National Superconducting Cyclotron Laboratory and

Department of Physics and Astronomy, East Lansing, MI 48824

E. K. Warburton

Brookhaven National Laboratory, Upton, New York 11973

Abstract

A new calculation of the predominantly isoscalar PNC matrix element between the $J^\pi T$ $0^+1, 0^-1$ ($E_x \approx 8.7$ MeV) states in ^{14}N has been carried out in a $(0+1+2+3+4)\hbar\omega$ model space with the Warburton-Brown interaction. The magnitude of the PNC matrix element of 0.22 to 0.34 eV obtained with the DDH PNC interaction is substantially suppressed compared with previous calculations in smaller model spaces but shows agreement with the preliminary Seattle experimental data. The calculated sign is opposite to that obtained

*permanent address: Department of Theoretical Physics, Institute of Atomic Physics, Bucharest Romania

experimentally, and the implications of this are discussed.

PACS numbers: 21.60.-n,21.60.Cs,27.20.+n,11.30.Er,21.10.Ky

Studies of low-energy parity nonconservation (PNC) in light nuclei have been developed to provide more reliable results on the hadron-meson weak-coupling constants which are of importance for our understanding of the quark behavior in nucleons under the influence of the fundamental interactions. These studies necessitate both very delicate experiments and very reliable nuclear structure calculations of the matrix elements for a correct extraction of the weak nucleon-meson coupling constants.

Most of the results on the experimental and theoretical PNC studies in light nuclei have been presented in the review by Adelberger and Haxton [1]. From the proposed cases during the last 25 years in light nuclei, four cases are thought to reliable for quantitative experimental and theoretical analysis. They involve parity-mixed doublets (PMD) [1] in ^{14}N, ^{18}F, ^{19}F and ^{21}Ne. Two others cases involving PMD's in ^{16}O [2] and ^{20}F [3] have been proposed recently. From the four mentioned cases, only that of ^{19}F has been measured with a result larger then the experimental error. The other cases have been measured with errors larger (^{18}F and ^{21}Ne) or near the result (^{14}N). However, the absolute values of the measured errors for ^{18}F and ^{21}Ne are so small that they impose severe constraints on the different contributions to the PNC matrix elements. These constraints combined with theoretical calculations indicate a discrepancy, which has not yet been completely resolved. Namely, if one interprets the small limit of the (experimentally) extracted PNC matrix element (< 0.029 eV) for ^{21}Ne as a destructive interference between the isoscalar and isovector contributions [1], then it is difficult to understand why the isovector contribution in ^{18}F is so small (< 0.09 eV) and the isoscalar + isovector contribution in ^{19}F is relatively so large (0.40 ± 0.10). The possibility of an amplification of the isovector contribution in ^{21}Ne is not supported by the actual structure calculations [1]. However, recent investigations [4] indicate that, in the ^{21}Ne case, the isoscalar contribution is very small (if not zero) and this could provide an explanation.

Another possibility for resolving this problem is to better study the isoscalar and isovector components separately. Continuous theoretical and experimental efforts have been undertaken in this direction. The only case predominantly isoscalar (no isovector contribution) is

the J^π,T $0^+1, 0^-1$ doublet ($E_x \approx 8.7$ MeV) in ^{14}N. Study of this doublet via the $^{13}C(\vec{p},p)^{13}C$ resonance scattering was proposed in 1984 [5] and preliminary experimental results were presented in Refs. [6,7]. The theoretical description of the scattering process is under control [5,8] and has been successfully tested for the regular observables. The predominantly isoscalar PNC matrix element (the isotensor part contributes $\sim 7\%$) has been calculated many times in different model spaces and with different Hamiltonians. The results vary from 1.39 eV in the ZBM ($0p_{1/2}$,$0d_{5/2}$,$1s_{1/2}$) model space [5] to 0.29 eV in a full $0p-1s0d$ (0+1+2)$\hbar\omega$ model space using the Kuo-Brown interaction [10].

The aim of this paper is to provide a new analysis of the PNC matrix element in ^{14}N based on a new Hamiltonian recently obtained by Warburton and Brown [11] and including also $3\hbar\omega$ and $4\hbar\omega$ configurations. This analysis is of importance for the support of the PNC experiments in ^{14}N [7,8] and to better understand how to improve the Hamiltonians for a more reliable description of the weak observables in light nuclei (A = 10-22).

In the last few years, important progress have been made in the improvement of the shell-model calculations with special emphasis on the description of the weak observables [12,13]. Recently, two new interactions have been developed by Warburton and Brown [11], which were designed to describe pure $\hbar\omega$ states in nuclei with A=10-22. For this purpose, all of the $0\hbar\omega$ and $1\hbar\omega$ and two-body matrix elements for the $0p-1s0d$ model space have been determined from a least squares fit to experimental binding energies. The 1s and 1f2p major shells were also included. For ^{16}O and ^{14}N, (0+2+4)$\hbar\omega$ calculations are now possible. In the first calculations for ^{16}O [12] it was found that a reduction (about 3 MeV) in the gap between the $0p$ and $1s0d$ major shells is necessary in order to account to for the spectrum of ^{16}O. More recently [13], it has been shown that this reduction compensates for the absent $\geq 6\hbar\omega$ configurations. That is, as is well known, the effective interaction and effective single-particle energies are model space dependent. Several choices for the $2\hbar\omega$ two-body matrix elements within the $0p-1s0d$ model space have been proposed, based upon the structure of the mixed (0+2+4)$\hbar\omega$ states in ^{16}O [13,14].

In order to investigate the sensitivity to various aspects of the truncation and interaction,

we have carried out the PNC calculation for ^{14}N using wave functions obtained with a variety of assumptions. Our shell-model calculations have been performed with the shell-model code OXBASH [15]. Spurious center of mass motion is removed by the usual method [16] of adding a center of mass Hamiltonian to the interaction. The first four major shells do not provide a completely nonspurious shell-model basis when more than $2\hbar\omega$ configurations are included. However, the effect of this spuriosity has been found it to be negligible.

For the first calculation discussed here we have used $(0+2)\hbar\omega$ configurations for the positive-parity states and $(1+3)\hbar\omega$ configurations for the negative-parity states. The WBT interaction from Ref. [11] was used for all two-body matrix elements. In order to reproduce the energy level spectrum of ^{14}N (see Fig. 1), the $0d_{5/2}$ single-particle energy (SPE) has been lowered by 1 MeV, the $0p_{1/2}$ SPE increased by 2.2 MeV and the $0p_{3/2}$ SPE increased by 0.7 MeV. These changes gives a very good spectrum for the $0^{\pm}$ and $1^{\pm}$ states in ^{14}N (see Fig. 1) and keeps the $\vec{l}\cdot\vec{s}$ splitting of the $0p$ states at a reasonable value. (It is recognized that these changes of the single-particle energies are perhaps arbitrary and not a unique method for reproducing the energy spectrum. However, below we will introduce other models and interactions.)

The PNC matrix element has been calculated in a one-body approximation. This method was pioneered by Michel [17], and recently justified and often used for the PNC calculations [1,18]. In this paper we have not used the one-body PNC potential derived in the Fermi gas model approximation (see Eqs. 17-20 of Ref. [1]). Instead, we have used an exact calculation of the one-body contribution to the PNC matrix element

$$< J^{\pi}T \mid V_{PNC} \mid J^{-\pi}T' >_{OB} = \sum_{n_1 l_1 j_1, n_2 l_2 j_2, t} \frac{C^{T' \; t \; T}_{M' \; \tau \; M}}{\sqrt{(2J+1)(2T+1)}}$$

$$\times < n_1 l_1 j_1 \parallel U^{(0t)}_{s.p.} \parallel n_2 l_2 j_2 > \text{OBTD}\ ((n_1 l_1 j_1)(n_2 l_2 j_2); 0t) \qquad (1)$$

where OBTD denotes the one-body-transition density and

$$< \alpha \mid U_{s.p.} \mid \beta > = \sum_{\delta \in core} < \alpha\delta \mid V_{PNC} \mid \beta\delta > - < \alpha\delta \mid V_{PNC} \mid \delta\beta > , \qquad (2)$$

is assumed. For ^{14}N, an interpolation between a ^{12}C core and a ^{16}O core has been performed. This method has been checked by comparing the one-body calculations (OB) with the full two-body (TB) calculations (see Table 1. *a* and *c*). The OB calculations give results with a precision of 2%, at least for the components of the V_{PNC} with the largest contribution to the matrix element, i.e.

$$V_{PNC}^{\Delta T=0} = -g_\rho h_\rho^\circ (1+\mu_v)\vec{\tau}_1 \cdot \vec{\tau}_2 \imath(\vec{\sigma}_1 \times \vec{\sigma}_2)\Big[\frac{\vec{p}}{2M}, \frac{\exp(-m_\rho r)}{4\pi r}\Big] \ . \tag{3}$$

in the isoscalar case (see Ref. [1] for notation).

The PNC matrix elements calculated with weak-coupling constants from different quark models (see Ref. [2] for notation and references) are presented in Table 1(*a*). The matrix elements were obtained using harmonic-oscillator wave functions with $\hbar\omega$ = 14.0 MeV. (Below we will address the important issues associated with loosely-bound wave functions.) The isotensor contribution has been calculated in the full TB approximation and is found to give about a 7% destructive contribution to the isoscalar matrix element. In all calculations discussed below this contribution has been added to the OB result. Our value of 0.489 eV obtained in the (0+1+2+3)$\hbar\omega$ model space with the WBT interaction and based on the DDH best values for the weak couplings, is to be compared with previous results of 1.39 eV from the ZBM ($0p_{1/2}$,$0d_{5/2}$,$1s_{1/2}$) model space with the REWIL interaction [5], 1.04 eV from the (0+1+2)$\hbar\omega$ model space [9], 0.56 eV from the (0+1+2)$\hbar\omega$ model space and the Millener-Kurath interaction [10], and 0.29 eV from the (0+1+2)$\hbar\omega$ model space with the Kuo-Brown interaction [10]. The experimental data [6,7,23] suggest a magnitude of about 0.38 ± 0.28 eV for the PNC matrix element. For comparison, a (1+2)$\hbar\omega$ calculation with the WBT interaction has been performed. The $(0^+1)_2$ state in the PMD has been assumed to be a pure $2\hbar\omega$ configuration, while the $(0^-1)_1$ state has been considered a pure $1\hbar\omega$ configuration. The calculated binding energies (no modification of the SPE) are quite close (-107.72 and -108.82 MeV for the 0^+1 and 0^-1 states respectively) and the PNC matrix element was found to be 1.24 eV for the DDH weak couplings.

It is interesting to analyze the contributions to the PNC matrix element in order to

understand the source of change when going to larger model spaces and the correlations with other calculated observables (e.g. the electromagnetic transition probabilities). It is convenient to rewrite the PNC matrix element, Eq. (1), in the following form

$$< (0^-1)_1 \mid V_{PNC}^{\Delta T=0} \mid (0^+1)_2 >= \sum_{\alpha\beta} \psi_{\alpha\beta} \mathcal{V}_{\alpha\beta} \equiv \sum_{\alpha\beta} \mathcal{C}_{\alpha\beta} \tag{4}$$

where α, β denotes the single-particle orbitals, $\psi_{\alpha\beta}$ is the one-body transition density (OBTD in Eq. (1) [15]) and $\mathcal{V}_{\alpha\beta}$ the single-particle matrix element of the one-body PNC potential (including the spin-isospin coefficient in front). The detailed contributions entering Eq. (4) are presented in Table 2 for the main component of $V_{PNC}^{\Delta T=0}$ [Eq. (3)]. The $\mathcal{C}_{\alpha\beta}$ and $\mathcal{V}_{\alpha\beta}$ are in MeV and they are given up to an dimensionless factor $-g_\rho h_\rho^\circ (1+\mu_v)/2$, which depends on the quark model. A general analysis of the important contributions to PNC matrix element has been made in Ref. [1]. Our specific results for ^{14}N are: a.) the main contribution comes from the $(\alpha\beta) = (0p_{1/2}1s_{/2})$ amplitude in all model spaces; this is the only contribution in the ZBM model space; b.) a spreading of the strength appears going to a larger model space, the $\psi_{0p_{1/2}1s_{1/2}}$ decreases, the effect of the other $(\alpha\beta)$ contributions is not more than 20 % and it is constructive in all cases (the destructive contribution coming from $\psi_{0p_{3/2}0d_{3/2}}$ is rather small); c.) the effect of the pairing forces in the destructive contribution $\psi_{\beta\alpha}$ (to $\psi_{\alpha\beta}$) can be seen only in the ZBM ($0p_{1/2}$,$0d_{5/2}$,$1s_{1/2}$) and $0p-1s0d$ (0+1+2+3)$\hbar\omega$ model spaces; it contributes 20% in the ZBM space and 40% in the larger (0+1+2+3)$\hbar\omega$ model space.

It was suggested in Ref. [1] that the E1 operators could behave in a similar way with respect to these destructive effects due to the fact that they are also odd under particle-hole conjugation; therefore they might represent a good test for the reliability of the wave functions with respect to the axial-charge matrix elements. In Table 3 some electromagnetic transition probabilities between $0^\pm$ and $1^\pm$ states in ^{14}N are included and compared with the recent experimental results. The B(M1) are very close to the experimental results of Zeps [6]. If one excludes the very small B(E1) transition $(1^-0)_1 \rightarrow (0^+1)_1$ all other B(E1) transitions are underestimated in the new calculations by a factor of 3 to 5; this means a

factor of 1.7 to 2.3 for the matrix element. Can we conclude that the PNC matrix element is underestimated by a similar factor? In order to address this question, it is important to look to the components of the E1 matrix elements and compare with those of the PNC matrix element. This analysis is presented in Table 4, for the transition $(0^+1)_2 \rightarrow (1^-0)_1$, where we have rewritten the E1 matrix element in the following form

$$< (1^-0)_1 \mid E1 \mid (0^+1)_2 > = \sum_{\alpha\beta} \psi_{\alpha\beta}\mathcal{E}_{\alpha\beta} \equiv \sum_{\alpha\beta} \mathcal{B}_{\alpha\beta} \ , \tag{5}$$

similar to Eq. (4). The $\psi_{0p_{1/2}1s_{1/2}}$ is still one of the main components, but the other important one comes from $\psi_{0p_{3/2}0d_{5/2}}$. Even if the $\psi_{0p_{3/2}0d_{5/2}}$ admixture is relatively small, its contribution is rather large due to a large single-particle matrix element, $\mathcal{E}_{\alpha\beta}$. The effect of $\psi_{\beta\alpha}$ is small and even constructive for the $\psi_{0p_{1/2}1s_{1/2}}$ component. So, the origin of the smallness of the E1 matrix element is due to the cancelation between $\psi_{0p_{1/2}1s_{1/2}}$ and $\psi_{0p_{3/2}0d_{5/2}}$ contributions which does not exist in the PNC case. One can conclude that in this case the smallness of the E1 matrix elements does not necessarily indicate an underestimation of the PNC matrix element.

Another important way to analyse the PNC matrix element is to consider different $n\hbar\omega \rightarrow (n \pm 1)\hbar\omega$ contributions. For such an analyses we have carried out calculations with various strong Hamiltonians and different methods to treat the effect of the higher $n\hbar\omega$ configurations. We have performed seven different calculations (see also the code labels in Table 1):

a - The WBT interaction [11] with the SPE modified as discussed above and with (0+1+2+3)$\hbar\omega$ configurations included.

b - Same as *a* except that $4\hbar\omega$ configurations are also included for the 0^+1 states.

c - The WBT interaction with a modified $0p - 1s0d$ gap ($\Delta\epsilon_{0p} = 0.9$ MeV, $\Delta\epsilon_{1s0d} = -1.1$ MeV) and with (0+1+2+3)$\hbar\omega$ configurations included.

d - Same as *c* except that $4\hbar\omega$ configurations are also included for the 0^+1 states.

e - The WBP interaction [11] with shifted energies [13] ($\Delta 2\hbar\omega = -6.0$ MeV, $\Delta 1\hbar\omega = -1.75$ MeV, $\Delta 3\hbar\omega = -7.25$ MeV) and with (0+1+2+3)$\hbar\omega$ configurations included.

f - Same as *e* except that the Bonn potential multiplied by 0.8 has been used for $2\hbar\omega$ 0p-1s0d cross-shell matrix elements [14] ($\Delta 2\hbar\omega = -6.$ MeV, $\Delta 1\hbar\omega = -2.5$ MeV, $\Delta 3\hbar\omega = -8.5$ MeV).

g - The Millener-Kurath interaction [19] with shifted energies ($\Delta 2\hbar\omega = -6.0$ MeV, $\Delta 1\hbar\omega = -2.5$ MeV, $\Delta 3\hbar\omega = -8.5$ MeV) and with (0+1+2+3)$\hbar\omega$ configurations.

The calculated PNC matrix elements are presented in Table 1. The corresponding spectra and the decompositions in $n\hbar\omega \rightarrow (n \pm 1)\hbar\omega$ contributions for some of these cases are presented in Figs. 1-6. The range of values for the DDH weak-coupling constants vary between 0.232 and 0.764 eV, with a average value of around 0.48 eV.

Table 5 presents the relative contributions to the wave functions of the $(0^+1)_2$ and $(0^-1)_1$ states coming from different n$\hbar\omega$ configurations. Table 6 presents the different $n\hbar\omega \rightarrow (n \pm 1)\hbar\omega$ contributions to the PNC matrix element (DDH weak couplings assumed). The $(0^+1)_2$ state is predominantly a $2\hbar\omega$ configuration. The $0\hbar\omega$ configuration is small (<10%) but the $0\hbar\omega$ -$1\hbar\omega$ contributions is rather large and opposite in sign as compared with the dominant $2\hbar\omega$ -$1\hbar\omega$ contribution. This is in fact the main mechanism of suppression of the PNC matrix element and it is very sensitive to the $0\hbar\omega$ content of the $(0^+1)_2$ wave function.

Another important point is the sign of the $2\hbar\omega \rightarrow 3\hbar\omega$ contribution. If the $\psi_{0p_{1/2}1s_{1/2}}$ component would be dominant for every contribution in the n$\hbar\omega \rightarrow (n\pm1)\hbar\omega$ series then the sign of this contribution should be negative and the PNC matrix element would be further suppressed. However, all calculations in Table 6 give a positive sign. This result is is very

sensitive to the mass dependence of the single-particle energies given by the interaction. All models in Table 6 correctly describe the experimental SPE order for ^{13}C ($1s_{1/2}$ $0d_{5/2}$). Another calculation with a version of the MK interaction which happened to give an opposite $0d_{5/2}$-$1s_{1/2}$ SPE order, gives an opposite sign for the $2\hbar\omega \rightarrow 3\hbar\omega$ contribution and, as a consequence, a very small PNC matrix element ($\sim$ 0.08 eV).

The $(0+2+4)\hbar\omega$ calculations for the 0^+1 states are not completely fixed. The inclusion of the $4\hbar\omega$ configurations depresses the $(0^+1)_2$ state by $\sim$ 3MeV. (No attempt to correct for this effect has been made.) The main result is that the $4\hbar\omega \rightarrow 3\hbar\omega$ contribution is positive and smaller than the $2\hbar\omega \rightarrow 3\hbar\omega$ one, suggesting a convergence of the series. The overall suppression of the PNC matrix element comes from the $0\hbar\omega$ contribution to the $(0^+1)_2$ wave function (9.8% in case b), and thus it is important to have a good description of the $0\hbar\omega$ contribution to the $(0^+1)_2$ wave function. One can try to fix this by looking to other observables, e.g. B(E1) and B(M1) transition probabilities. Different contributions to B(E1) matrix elements for the $(0^+1)_2 \rightarrow (1^-0)_1$ transition are presented in Table 8. One can see that the dominant contributions are $0\hbar\omega \rightarrow 1\hbar\omega$ and $2\hbar\omega \rightarrow \hbar\omega$ these are in phase and hence are not very sensitive to the $0\hbar\omega$ contribution to the $(0^+1)_2$ wave function.

The B(M1) transitions $(0^+1)_2 \rightarrow (1^+0)_{1,2}$ which are, of course, all $n\hbar\omega \rightarrow n\hbar\omega$ appear to be much more relevant. The various $n\hbar\omega$ contributions to the B(M1) matrix elements are presented in Table 7. The $0\hbar\omega$ and $2\hbar\omega$ contributions are opposite in sign and thus contribute destructively to the total B(M1). The $0\hbar\omega$ contributions are not exactly proportional to the total amount of the $0\hbar\omega$ configuration of the $(0^+1)_2$ wave function. However, it is clear that the cases with a relatively higher $0\hbar\omega$ content (b, d, f, g) give a relatively small B(M1) value as compared with the experimental data in Table 3. From this one may estimate approximately 3-5% $0\hbar\omega$ content of the $(0^+1)_2$ wave function and $\sim$ -(0.350 - 0.450) eV for the $0\hbar\omega$ -$1\hbar\omega$ contribution to the PNC matrix element.

Another ingredient which is often important for the PNC matrix element is the effect of the derivative operator (see Eq. (3)) on the tails of the single-particle wave functions (SPWF) [1]. The use of Woods-Saxon (WS) SPWF decrease the matrix element as compared with its

value calculated with harmonic oscillator (HO) SPWF. However, we make two observations i.) The derivative operator does not act directly on the SPWF but rather on the matrix element of the short range form factor, $[\partial/\partial r(exp(-m_\rho r)/r)]$. ii.) It is clear that the use of the WS SPWF will change the value of the PNC matrix element, especially when some states in the WS basis are unbound or nearly unbound.

We have estimated the effect of the nearly unbound $1s_{1/2}$ WS state on the dominant $0p_{1/2} \rightarrow 1s_{1/2}$ contribution to the PNC matrix element. The $1s_{1/2}$ proton level is unbound by 0.4 MeV in ^{13}N and is slightly bound by 0.1 MeV in ^{17}F. For neutrons, the same level is bound by 1.9 MeV in ^{13}C and by 3.25 MeV in ^{17}O. We have chosen a -0.1 MeV value for the $1s_{1/2}$ proton SPE and -2.0 MeV for the neutron SPE. The comparable values for the $0p_{1/2}$ orbit are -2.5 MeV for protons and -5.0 MeV neutrons. The WS SPWF are obtained by adjusting the WS well depth to reproduce the above binding energies. we have found a suppression of the dominant $0p_{1/2} \rightarrow 1s_{1/2}$ contribution to the PNC matrix element of 37% in the case of protons and 28% for neutrons, an average of 32%.

In the end a few comments concerning the sign of the PNC observable, the longitudinal analyzing power. The sign found in the experiment [6,7] is opposite from our calculations as well as from the initial prediction [5]. The sign of the calculated observable depends on the product signs associated with the PNC matrix element and the spectroscopic amplitudes, which describe the proton decay of the compound states in ^{14}N. As in the previous calculation, the dominant contribution to the PNC matrix element comes from the 1-2$\hbar\omega$ transition (see Figs. 2-3). Moreover, the spectroscopic factors appear to be stable quantities for this case. For instance in case (c), we obtained for C_{0^+} (see Ref. [5] for notations) a value of $0.226/\sqrt{2}$ - to be compared with $0.299/\sqrt{2}$ in ZBM case [5] - and $0.977/\sqrt{2}$ for C_{0^-} (to be compared with $1/\sqrt{2}$ for ZBM). The $n\hbar\omega$ decompositions of the spectroscopic factors gives $0.210/\sqrt{2}$ for the $^{14}N(0^+1)_2 0\hbar\omega \rightarrow^{13} C\ g.s.\ 0\hbar\omega$, $0.016/\sqrt{2}$ for $^{14}N(0^+1)_2\ 2\hbar\omega \rightarrow^{13} C\ g.s.\ 2\hbar\omega$, $0.827/\sqrt{2}$ for $^{14}N(0^-1)_2\ 1\hbar\omega \rightarrow^{13} C\ g.s.\ 0\hbar\omega$ and $0.150/\sqrt{2}$ for the $^{14}N(0^-1)_2\ 1\hbar\omega \rightarrow^{13} C\ g.s.\ 2\hbar\omega$. The contributions from different $n\hbar\omega$ transitions are in phase for both spectroscopic factors so they are more stable quantities than the PNC

matrix element. The widths of the 0^+, 0^- states calculated with these spectroscopic factors and the method described in Ref. [5] are 5.2 and 1020 keV respectively. They are in relatively good agreement (if one have in mind that the width is proportional to the matrix element squared) with the experimentally extracted ones [24]: 3.8 ± 0.3 keV and 410 ± 20 keV.

The sign of the isoscalar PNC matrix element has an interesting history. The earliest calculations based upon the factorization approximation gave a sign which was consistently opposite to that found experimentally in the ^{19}F and $\vec{p} + p$ experiments [21,22]. Later, estimates of the quark and sum-rule contributions for the nucleon-nucleon PNC interactions were added and were found to change the sign of the isoscalar PNC interaction, bringing the sign in agreement with the experiment [21,22]. The actual sign from the ^{19}F experiment is not definite because it relies on calculating the correct sign for a very weak E1 matrix element. Thus we have at present three pieces of data: (a) $\vec{p}+p$ scattering which prefers the DDH sign, (b) the ^{19}F experiment which prefers the DDH sign but is not certain and (c) the ^{14}N experiment which prefers the factorization approximation. It is difficult to reconcile (a) and (c). Perhaps the reconciliation of (a) and (c) will require "in medium" modification of the isoscalar PNC weak coupling constants, but further and more accurate calculations and experiments will be needed to clarify this puzzle.

In conclusion, new calculations of the predominantly isoscalar PNC matrix element between the $(0^+1)_2, (0^-1)_1$ states in ^{14}N have been performed in a $(0+1+2+3+4)\hbar\omega$ model space using new Hamiltonians. A new method to calculate the PNC matrix elements in an one-body approximation has been proposed and shown to give reliable results as compared with the full two-body calculations; this method proves to be very useful for calculations in larger model space, e.g. $(0+1+2+3+4)\hbar\omega$. The most reasonable range of values for the PNC matrix element was found to be 0.22 to 0.34 (a 32% WS suppression included), which is in reasonable agreement with a magnitude of about 0.38 ± 0.28 eV deduced from experiment [6,7,23] (even with the upper limit given by the error, if one dismiss the experimental result as accurate). Our range of values are suppressed by a factor of 3-4 with respect to the ZBM

$(0p_{1/2},0d_{5/2},1s_{1/2})$ calculations. This suppression comes mainly from the decrease of the $\psi_{0p_{1/2}1s_{1/2}}$ OBTD and from a stronger cancellation due to the particle-hole conjugate transition densities. All calculated E1 transition probabilities between $0^{\pm}, 1^{\pm}$ states in ^{14}N are smaller than the experimental results but, the mechanism of suppression for the E1 matrix elements is different than for the PNC matrix element. The analysis of the $n\hbar\omega \rightarrow (n\pm1)\hbar\omega$ contributions put in evidence the importance of the $0\hbar\omega$ content of the $(0^+1)_2$ wave function. This part can be to some extent fixed by the B(M1) transition probabilities. The relative sign of the $2\hbar\omega \rightarrow 3\hbar\omega$ contributions appear to be fixed as positive but its magnitude remains as somewhat uncertain. The effect of higher ($>3\hbar\omega$) configurations deserves further study as well as the convergence of the $n\hbar\omega \rightarrow (n \pm 1)\hbar\omega$ series.

The authors want to thank Dr. V.J. Zeps for valuable suggestions concerning the content of the manuscript and for allowing them to use the new experimental electromagnetic transitions strengths before publication. M.H. would like to thank the Alexander von Humboldt Foundation for a fellowship during which this work has been done. B.A.B. would like to acknowledge support from the Alexander van Humboldt Foundation and NSF grant 90-17077.

REFERENCES

[1] E.G. Adelberger and W.C. Haxton, Ann. Rev. Nucl. Part. Sci. **35**, 501 (1985).

[2] N. Kniest, M. Horoi, O. Dumitrescu and G. Clausnitzer, Phys. Rev. **C44**, 491 (1991).

[3] M. Horoi and G. Clausnitzer, Phys. Rev. **C48**, R522(1993).

[4] M. Horoi, G. Clausnitzer, B.A. Brown and E.K. Warburton, in Proceedings of the NATO Advanced Study Institute Summer School, Predeal August 25 - September 6, 1993, Eds. W. Scheid and A. Sandulescu, Plenum Press 1994.

Verhandlungen der Deutschen Physikalischen Gesselschaft Mainz, 21-26 March, 1993, p.560.

[5] E.G. Adelberger, P. Hoodbhoy and B.A. Brown, Phys. Rev. **C30**, 456 (1984); Phys. Rev. **C33**, 1946 (1986).

[6] V.J. Zeps et al., A.I.P. Conf. Proc. **176**, 1098 (1989).

[7] V.J. Zeps, PhD thesis, University of Washington 1989, unpublished.

[8] M. Horoi, M. Preiss, R. Baumann and G. Clausnitzer, to be published.

[9] J. Dubach and W.C. Haxton, unpublished work 1980, quoted in Ref. [1].

[10] C. Johnson and W.C. Haxton, unpublished work 1988, quoted in Ref. [7].

[11] E.K. Warburton and B.A. Brown, Phys. Rev. **C46**, 923 (1992).

[12] W.C. Haxton and C. Johnson, Phys. Rev. Lett. **65**, 1325 (1990).

[13] E.K. Warburton, B.A. Brown and D.J. Millener, Phys. Lett. **293B**, 7 (1992).

[14] B.A. Brown and E. K. Warburton, unpublished.

[15] B.A. Brown et al., MSUNSCL Report, **524** (1988).

[16] D.H. Gloeckner and R.D. Lawson, Phys. Lett. **53B**, 313 (1974).

P.R. Rath, A. Faessler, H. Muther and A. Watt, J. Phys. **G 16**, 245 (1990).

[17] F.C. Michel, Phys. Rev. **B133**, 329 (1964).

[18] S.E. Koonin, C.W. Johnson and P. Vogel, Phys. Rev. Lett. **69**, 1163 (1992).

[19] D. J. Millener and D. Kurath, Nucl. Phys. **A255**, 315 (1975).

[20] F. Ajzenberg-Selove, Nucl. Phys. **A523**, 1 (1991).

[21] B. Desplanques, J. F. Donoghue and B. R. Holstein, Ann. Phys. (N. Y.) **124**, 449(1980).

[22] B. R. Holstein, Can. J. Phys. **66**, 508(1988).

[23] V. J. Zeps, E. G. Adelberger, A. García, C.A. Gossett, H. E. Swanson, W.Haeberli, P.A. Quin and J. Sromicki, to be published

[24] P.B. Fernandez, C.A. Gossett, J.L. Osborne, V.J. Zeps and E.G Adelberger, Bull. Am. Phys. Soc. **30**, 1161(1985).

Figure captions

Figure 1 Experimental and calculated $0^{\pm}, 1^{\pm}$ levels in ^{14}N. The calculation is that of model a obtained with the WBT interaction [11] and modified SPE within the $(0+1+2+3)\hbar\omega$ model space as described in the text.

Figure 2 Decomposition of the PNC matrix element into the contributions coming from different $n\hbar\omega$ components of the wave functions. The calculation is that of model a and the DDH weak-coupling constants have been used. Units are eV.

Figure 3 Same as Figure 2 but with model b where $4\hbar\omega$ configurations are also included.

Figure 4 Same as Figure 1 but with model c.

Figure 5 Same as Figure 1 but with model e.

Table 1 Magnitude of the PNC matrix element calculated with the various strong interactions [11], different model spaces, and different models of the weak-coupling constants (see Ref. [2] for the weak interaction notation and references). Units are eV. Code labels are further explained in the text.

Interaction	Code	Model space	PNC	Weak-Coupling Models			
				DDH	AH	DZ	KM
WBT	a	$(0+1+2+3)\hbar\omega$	OB	0.487	0.372	0.421	0.278
SPE	a	$(0+1+2+3)\hbar\omega$	TB	0.483	0.366	0.413	0.269
modification	b	$(0+1+2+3+4)\hbar\omega$	OB	0.233	0.164	0.190	0.1 27
WBT	c	$(0+1+2+3)\hbar\omega$	OB	0.764	0.565	0.620	0.418
gap	c	$(0+1+2+3)\hbar\omega$	TB	0.732	0.549	0.620	0.400
modification	d	$(0+1+2+3+4)\hbar\omega$	OB	0.497	0.366	0.413	0.2 72
WBP	e	$(0+1+2+3)\hbar\omega$	OB	0.502	0.370	0.418	0.275
	e	$(0+1+2+3)\hbar\omega$	TB	0.492	0.371	0.417	0.269
WBP + 0.8 Bonn	f	$(0+1+2+3)\hbar\omega$	OB	0.351	0.260	0.292	0.193
MK	g	$(0+1+2+3)\hbar\omega$	OB	0.331	0.246	0.276	0.181

Table 2 Components of the PNC matrix element entering Eq. (4) as described in text.

			ZBM		(1+2)$\hbar\omega$		(0+1+2+3)$\hbar\omega$	
α	β	$\mathcal{V}_{\alpha\beta}$	$\psi_{\alpha\beta}$	$\mathcal{C}_{\alpha\beta}$	$\psi_{\alpha\beta}$	$\mathcal{C}_{\alpha\beta}$	$\psi_{\alpha\beta}$	$\mathcal{C}_{\alpha\beta}$
$0p_{1/2}$	$1s_{1/2}$	0.171	1.193	0.204	0.717	0.1226	0.510	0.0871
$1s_{1/2}$	$0p_{1/2}$	-0.171	0.259	-0.044			0.235	-0.0402
$1s_{1/2}$	$0p_{1/2}$	-0.196			-0.082	0.0161	-0.045	0.00881
$0p_{1/2}$	$1s_{1/2}$	0.196					-0.0006	-0.0001
$0p_{3/2}$	$0d_{3/2}$	-0.213			0.004	-0.0009	0.044	-0.0102
$0d_{3/2}$	$0p_{3/2}$	0.213					0.028	0.0063
$1s_{1/2}$	$2p_{1/2}$	-0.169			0.072	0.0122	-0.015	0.0025
$2p_{1/2}$	$1s_{1/2}$	0.169					0.015	0.0025

Table 3 Experimental and calculated electromagnetic transition probabilities, B(M1) and B(E1), between $0^{\pm}, 1^{\pm}$ states in ^{14}N. Units are μ_N^2 and e^2fm^2, respectively.

		Experiment		Theory	
transition	type	AjS [20]	Zeps [23]	ZBM	(0+1+2+3)$\hbar\omega$
$(0^+1)_2 \rightarrow (1^+0)_1$	M1	0.159	0.05±0.005	0.32	0.031
$\rightarrow (1^+0)_2$	M1	1.056	1.05±0.1		0.572
$\rightarrow (1^+0)_3$	M1	12.71	12.2±1.2	12.7	11.31
$\rightarrow (1^-0)_1$	E1	0.0258	0.0161±0.0019	0.16	0.0042
$(0^-1)_1 \rightarrow (1^+0)_1$	E1	0.0636±0.0187	0.0355±0.0028	0.086	0.015
$(1^-0)_1 \rightarrow (0^+1)_1$	E1	$((0.42\pm0.19)\cdot10^{-3})$			$0.44\cdot10^{-2}$
$(1^-1)_1 \rightarrow (1^+0)_1$	E1	$(1.8\pm0.45)\cdot10^{-2}$	$(1.23\pm0.09)\cdot10^{-2}$		$0.62\cdot10^{-2}$
$\rightarrow (1^+0)_2$	E1	$(2.1\pm0.45)\cdot10^{-2}$	$(1.47\pm0.12)\cdot10^{-2}$		$0.46\cdot10^{-2}$

Table 4 Components of the E1 matrix element entering Eq. (5) for the $(0^+1)_2 \rightarrow (1^-0)_1$ transition.

			ZBM		(0+1+2+3)$\hbar\omega$	
α	β	$\mathcal{E}_{\alpha\beta}$	$\psi_{\alpha\beta}$	$\mathcal{B}_{\alpha\beta}$	$\psi_{\alpha\beta}$	$\mathcal{B}_{\alpha\beta}$
$0p_{1/2}$	$1s_{1/2}$	0.485	0.6886	0.334	0.2804	0.136
$1s_{1/2}$	$0p_{1/2}$	0.485	0.1493	0.072	0.1191	0.057
$0p_{3/2}$	$0d_{5/2}$	-1.455			0.0514	-0.0749
$0d_{5/2}$	$0p_{3/2}$	1.455			0.0029	0.00415

Table 5 Relative contributions of the $n\hbar\omega$ excitations to the wave functions of $(0^+1)_2$ and $(0^-1)_1$ states in ^{14}N. Code labels correspond to the cases in Table 1.

Code	$J^\pi T$	$0\hbar\omega$	$1\hbar\omega$	$2\hbar\omega$	$3\hbar\omega$	$4\hbar\omega$
	0^+1	0.047		0.953		
a	0^-1		0.855		0.145	
	0^+1	0.098		0.773		0.129
b	0^-1		0.855		0.145	
	0^+1	0.031		0.969		
c	0^-1		0.838		0.162	
	0^+1	0.073		0.763		0.164
d	0^-1		0.838		0.162	
	0^+1	0.061		0.939		
e	0^-1		0.818		0.182	
	0^+1	0.078		0.922		
f	0^-1		0.782		0.218	
	0^+1	0.050		0.950		
g	0^-1		0.876		0.124	

Table 6 The $n\hbar\omega \rightarrow (n \pm 1)\hbar\omega$ contributions to the PNC matrix element (DDH weak couplings assumed) for various cases studies (described by code labels). Units are eV.

Code	$0\hbar\omega$ -$1\hbar\omega$	$2\hbar\omega \rightarrow 1\hbar\omega$	$2\hbar\omega \rightarrow 3\hbar\omega$	$3\hbar\omega \rightarrow 4\hbar\omega$
a	-0.440	0.793	0.172	
b	-0.638	0.732	0.121	0.079
c	-0.347	0.941	0.228	
d	-0.538	0.804	0.152	0.113
e	-0.453	0.764	0.222	
f	-0.530	0.717	0.190	
g	-0.344	0.669	0.032	

Table 7 $n\hbar\omega \rightarrow n\hbar\omega$ contributions to the relevant M1 matrix elements in units of μ_N. Last column contains the calculated B(M1) (μ_N^2). Relative contributions of $n\hbar\omega$ excitations to the wave functions are also given.

		$(0^+1)_2$		$(1^+0)_n$		M1 matrix element			B(M1)
Transition	Code	$0\hbar\omega$	$2\hbar\omega$	$0\hbar\omega$	$2\hbar\omega$	$0\hbar\omega$	$2\hbar\omega$	total	
$(0^+1)_2$	a	0.047	0.953	0.765	0.235	-0.108	0.284	0.176	0.031
$\rightarrow (1^+)_1$	b	0.098	0.773	0.765	0.235	-0.160	0.270	0.110	0.012
	c	0.031	0.969	0.747	0.253	-0.162	0.452	0.290	0.084
	d	0.073	0.763	0.747	0.253	-0.263	0.382	0.119	0.014
	e	0.061	0.939	0.719	0.281	-0.274	0.546	0.273	0.074
	f	0.078	0.922	0.735	0.265	-0.198	0.250	0.051	0.0026
	g	0.050	0.950	0.809	0.191	-0.140	0.238	0.108	0.012
$(0^+1)_2$	a	0.047	0.953	0.676	0.324	-0.485	1.242	0.757	0.572
$\rightarrow (1^+)_2$	b	0.098	0.773	0.676	0.324	-0.160	0.270	0.110	0.012
	c	0.031	0.969	0.698	0.302	-0.375	0.999	0.625	0.390
	d	0.073	0.763	0.698	0.302	-0.263	0.382	0.119	0.014
	e	0.061	0.939	0.651	0.349	-0.488	1.192	0.704	0.495
	f	0.078	0.922	0.610	0.390	-0.552	1.252	0.707	0.490
	g	0.050	0.950	0.727	0.273	-0.476	0.852	0.376	0.141

Table 8 $n\hbar\omega \rightarrow (n \pm 1)\hbar\omega$ contributions to the $(0^1)_2 \rightarrow (1^-0)_1$ E1 matrix elements in units efm. Last column contains the calculated B(E1) (e^2fm^2). Relative contributions of $n\hbar\omega$ excitations to the wave functions are also given.

	$(0^+1)_2$		$(1^-0)_1$		E1 matrix element					B(E1)
Code	$0\hbar\omega$	$2\hbar\omega$	$1\hbar\omega$	$3\hbar\omega$	$0 \rightarrow 1\hbar\omega$	$2 \rightarrow 1\hbar\omega$	$2 \rightarrow 3\hbar\omega$	$4 \rightarrow 3\hbar\omega$	total	
a	0.047	0.953	0.839	0.161	0.026	0.053	-0.014		0.065	0.0042
b	0.098	0.773	0.839	0.161	0.037	0.040	-0.014	0.0001	0.063	0.0040
c	0.031	0.969	0.828	0.172	0.015	0.055	-0.017		0.053	0.0029
d	0.073	0.763	0.828	0.172	0.024	0.033	-0.016	0.0014	0.039	0.0015
e	0.061	0.939	0.876	0.124	0.013	0.038	-0.013		0.039	0.0016
f	0.078	0.922	0.778	0.222	0.016	0.040	-0.006		0.051	0.0026
g	0.050	0.950	0.876	0.124	0.041	0.067	0.011		0.119	0.0142

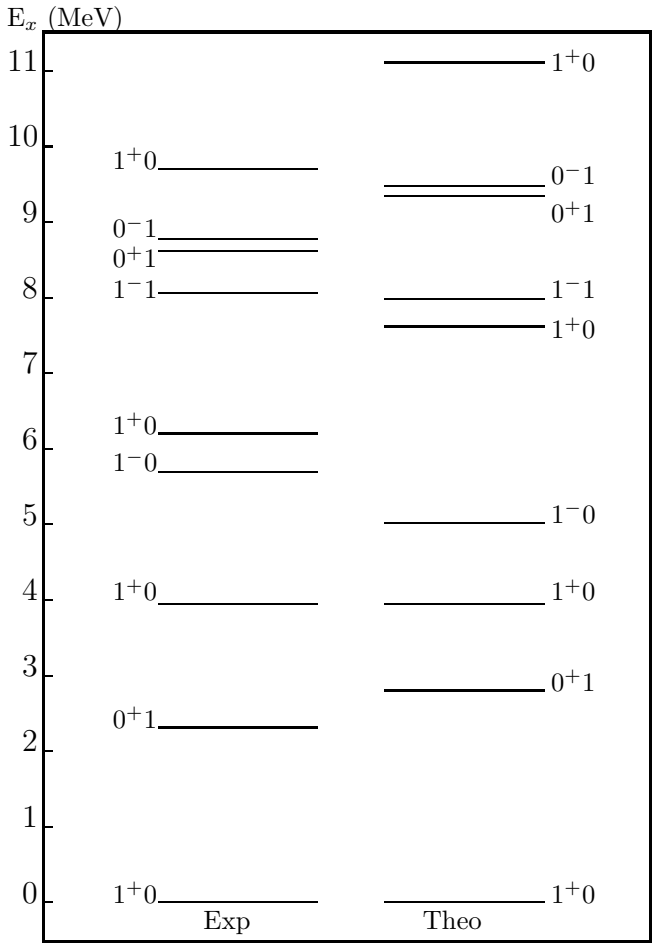
E$_x$ (MeV)
11
10
9
8
7
6
5
4
3
2
1
0
1^+0
1^+0
0^-1
0^+1
1^-1
1^+0
1^-0
1^+0
0^+1
1^+0
Exp
1^+0
0^-1
0^+1
1^-1
1^+0
1^-0
1^+0
0^+1
1^+0
Theo

Figure 1.

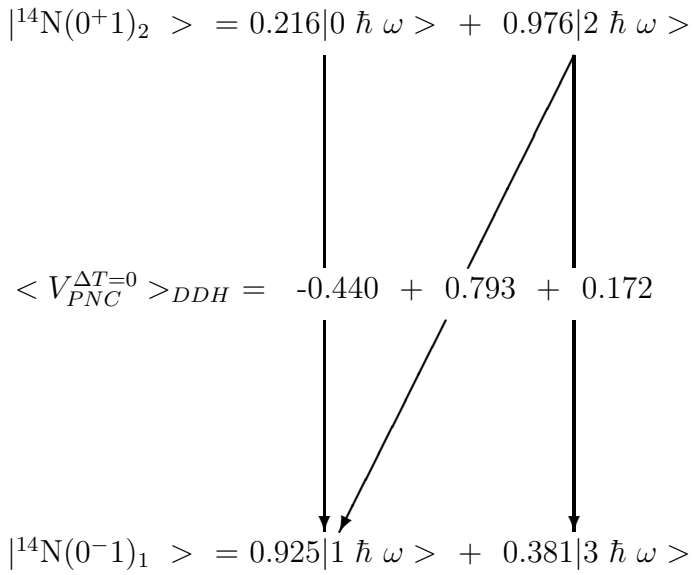

Figure 2.

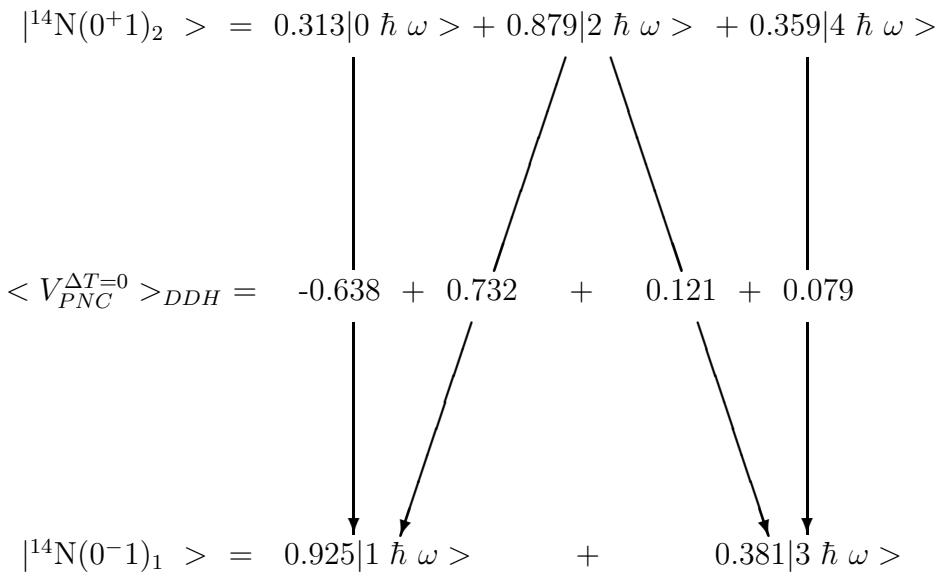

Figure 3.

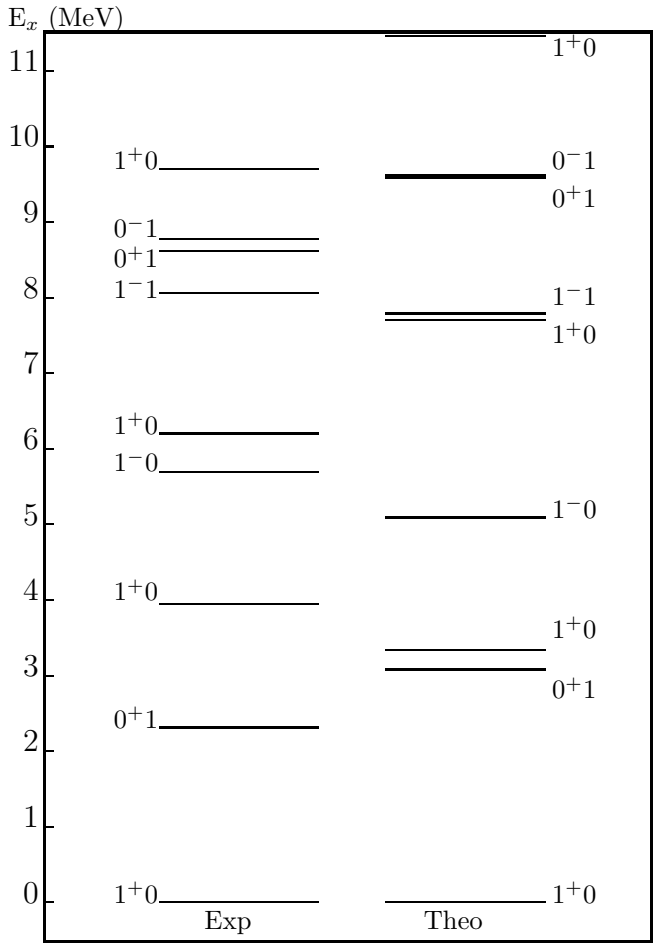
E$_x$ (MeV)
11
10
9
8
7
6
5
4
3
2
1
0
1^+0
0^-1
0^+1
1^-1
1^+0
1^-0
1^+0
0^+1
1^+0
1^+0
0^-1
0^+1
1^-1
1^+0
1^-0
1^+0
1^+0
0^+1
1^+0
Exp
Theo

Figure 4.

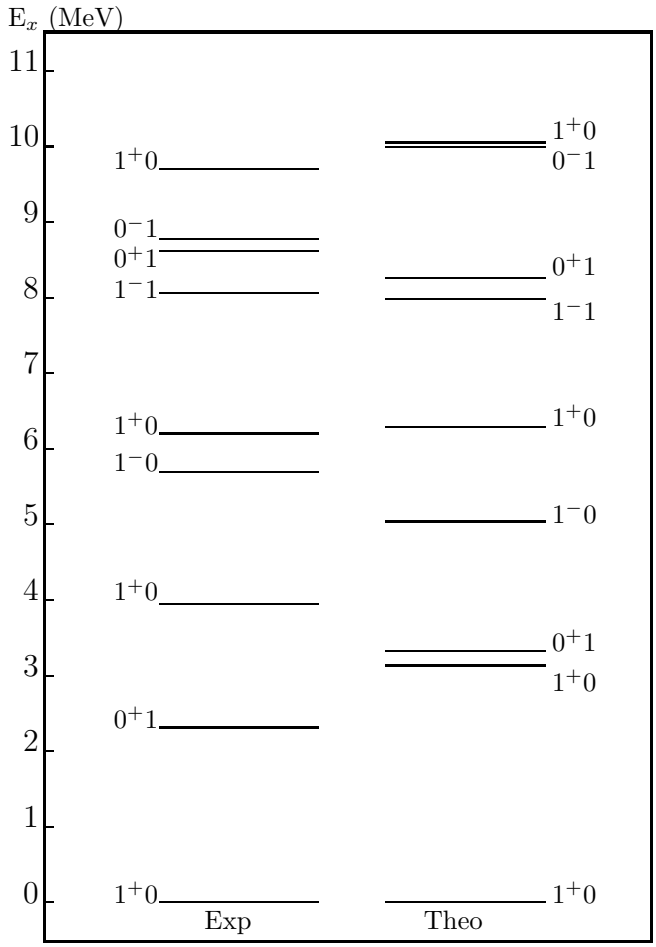
E$_x$ (MeV)
11
10
9
8
7
6
5
4
3
2
1
0
1^+0
0^-1
0^+1
1^-1
1^+0
1^-0
1^+0
0^+1
1^+0
1^+0
0^-1
0^+1
1^-1
1^+0
1^-0
0^+1
1^+0
1^+0
Exp
Theo

Figure 5.